Eur. Phys. J. D **25**, 31–40 (2003)
DOI: 10.1140/epjd/e2003-00216-4

THE EUROPEAN PHYSICAL JOURNAL D

Photodissociation and photoionization of sodium coated C_{60} clusters

M. Pellarin[1,a], E. Cottancin[1], J. Lermé[1], J.L. Vialle[1], M. Broyer[1], F. Tournus[2], B. Masenelli[2], and P. Mélinon[2]

[1] Laboratoire de Spectrométrie Ionique et Moléculaire[b], 43 boulevard du 11 novembre 1918, 69622 Villeurbanne Cedex, France
[2] Laboratoire de Physique de la Matière Condensée et Nanostructures[c], 43 boulevard du 11 novembre 1918, 69622 Villeurbanne Cedex, France

Received 3rd March 2003 / Received in final form 7 May 2003
Published online 17 July 2003

Abstract. $(C_{60})_mNa_n$ clusters are produced in a tandem laser vaporization source and analyzed by photoionization and photofragmentation time-of-flight mass spectroscopy. At low sodium coverage, the special behavior of $(C_{60})_{m=1,2}Na_n$ clusters ($n \leq 6m$) is consistent with a significant electron transfer from the first six adsorbed atoms towards each of the C_{60} fullerenes and an ionic-like bonding in this size range. However, the stability of the $(C_{60})Na_3^+$ cation is found much more pronounced than the one of $(C_{60})Na_7^+$ predicted to be a magic size under the hypothesis of a full charge transfer from the metal atoms to the C_{60} molecule. When more sodium atoms are present, metal-metal bonds tend to become preponderant and control the cluster properties. Relative to the number of sodium atoms, an odd-even alternation in their stability is explained by the high dissociation rates for even-numbered clusters. The even clusters evaporate neutral sodium atoms whereas odd ones prefer to evaporate Na_2 molecules. The hypotheses for the growth of a sodium droplet that does not wet the fullerene surface or for the formation of a concentric metallic layer are discussed in the light of this study.

PACS. 36.40.Qv Stability and fragmentation of clusters – 36.40.Mr Spectroscopy and geometrical structure of clusters

1 Introduction

The bulk intercalation compounds of C_{60} with metals have attracted much interest because of their unique properties and especially the superconductivity of some alkali or alkaline earth doped fullerides [1]. The fundamental aspects of metal-C_{60} interactions can be advantageously investigated in gas phase experiments on individual C_{60} clusters coated with the corresponding metallic species. For a large amount of metal, experimental findings give evidence for the formation of a spherical shell around the central fullerene [2,3]. This is now clear for alkaline-earth elements where the cluster structure is ruled by the geometric packing of atoms in concentric layered shells [4]. In the case of cesium, ionization potential measurements [5] and photoabsorption spectra [6] of $(C_{60})Cs_n$ clusters can be qualitatively explained by the jellium-like behavior of a metallic shell at the C_{60} surface. This core-shell structure is supported by theoretical studies [5,7,8] even if the agreement between theory and experiment is not quantitatively perfect. When the number of atoms is not sufficient to complete a first atomic layer, the situation is much different. The properties of the coated fullerene can no longer be described by those of a metallic part just slightly perturbed by the C_{60}. It must be considered as a molecular system where the C_{60}-metal interactions may dominate the metal-metal ones. In this respect, the charge transfer processes between the first attached atoms and the C_{60} are of main importance. This has been established for rubidium [3,9], potassium [9–12] and lithium [11,13–15]. The case of sodium compounds is the most debated. The conclusions drawn from different experimental studies on these systems are somewhat conflicting [10,16–18]. This point will be discussed in the following. On the other hand, a few theoretical studies have been devoted to this issue [11,19,20]. They are evoked in the most recent work by Hamamoto *et al.* [21] which gives fruitful information concerning the degree of charge transfer between the metal and the fullerene, the arrangement of atoms at the fullerene surface or the number of atoms required for the metallic behavior to be effective. Moreover, Roques *et al.* [22] have very recently developed an empirical potential method allowing the exploration of a large number of structures for $(C_{60})Na_n$ clusters so as to get information about the segregation of the metallic part as a function of their size.

In this paper, we will discuss the photo-induced dissociation pathways of some size-selected sodium-C_{60}

[a] e-mail: pellarin@lasim.univ-lyon1.fr
[b] UMR 5579 du CNRS
[c] UMR 5586 du CNRS

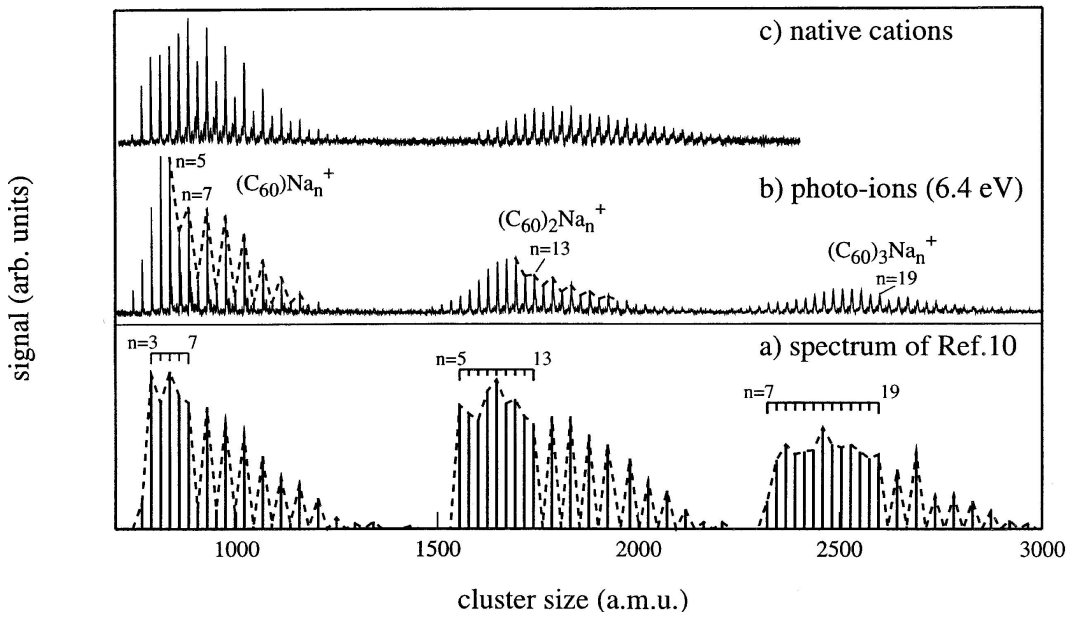

Fig. 1. (a) High laser fluence photoionization mass spectrum taken from [10] (bottom); (b) mass spectrum of neutral species photo-ionized with an ArF laser at 6.4 eV and at moderate fluence (middle); (c) mass spectra of $(C_{60})Na_n^+$ clusters directly produced by the source (top). An odd-even alternation in the cluster abundances is indicated by dotted lines.

compounds. The observed features are expected to bring additional information about their structure so as to complement previous studies on this issue [9,10,17,18].

2 Experimental set-up

Sodium-C_{60} complexes are produced in a double-target laser vaporization source previously used in the study of silicon-C_{60} mixed clusters [23]. One target consists of a metallic sodium rod and the other is processed in the form of a disk by pressing a high purity (99%) C_{60} powder. Both targets are independently vaporized by two frequency-doubled Nd:YAG lasers. The laser beams are perpendicular one to each other and to the axis of the chamber in such a way that the sodium plasma and the C_{60} vapor are efficiently mixed. Because of a fast surface oxidization of the sodium rod during the transfer to the source chamber, it is necessary to clean it with the vaporization laser before performing measurements.

$(C_{60})_m Na_n$ neutral clusters can be ionized by an ArF excimer laser (6.4 eV) or a dye laser pumped by an XeCl excimer laser in order to perform near threshold photoionization spectroscopy of these species at selected photon energies. The size distributions are analyzed in a reflectron time-of-flight spectrometer (RTOFS). We have also carried out photofragmentation measurements on size selected clusters by taking advantage of the natural tandem TOF configuration of the reflectron spectrometer [24]. The clusters are size-selected by a pulsed electrostatic gate and photoexcited by the beam of a XeCl excimer laser in the field free region of the RTOFS, at the first focal point of the system. Its location is adjusted by tuning the ratio between the acceleration and extraction electric fields in the ion source and is a compromise to obtain a correct resolution both for the entire RTOFS ($M/\Delta M = 2000$) and for the mass selector ($M/\Delta M = 100$). The size resolution is mainly limited by the mass peak broadening due to the isotopic distribution of carbon but exact mass coincidences between pure or oxidized $(C_{60})_m Na_n$ clusters with different compositions are forbidden. If some oxides are partly selected with pure clusters when performing photofragmentation experiments, the spatial sharpness of the laser allows to excite selectively the bare species. All these experiments can be performed on photoionized clusters or clusters directly produced by the source as cations. We prefer the first solution because of a better signal stability and a lower oxidization of the detected clusters. In the case of photoionized clusters that may undergo an extra warming at the acceleration stage, it is also possible to detect their delayed unimolecular dissociation without resorting to the fragmentation laser.

3 Results

3.1 Mass spectroscopy

Figure 1 shows a comparison between a mass spectrum of cationic clusters directly produced by the source (Fig. 1c) and a mass spectrum of neutral clusters photoionized with an ArF excimer laser (Fig. 1b). The odd-even alternation in the relative yield of sodium coated C_{60} clusters is more pronounced for photo-ionized species as discussed in the next section but can also be guessed for cations. The overall shape of the size distributions and the degree of fullerene coating with sodium are very sensitive to the source operation parameters. Oxides or hydroxides are

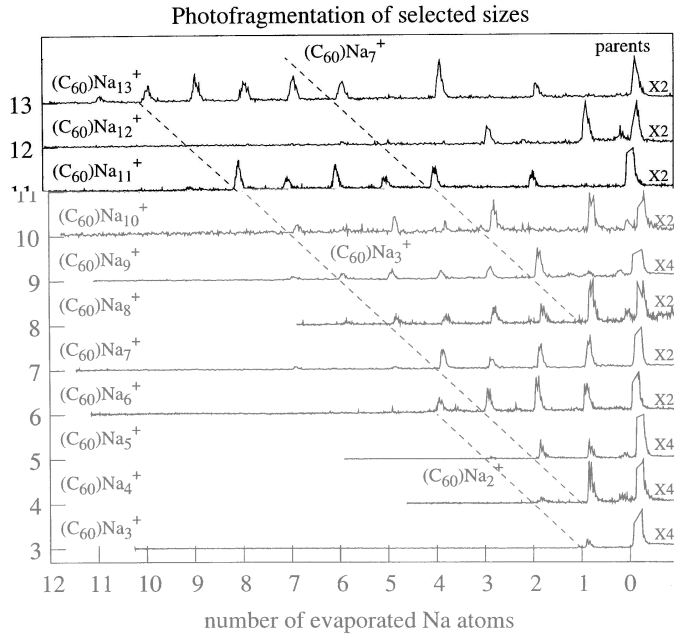

Fig. 2. Photofragmentation spectra of $(C_{60})Na_n^+$ clusters. The oblique doted lines give the expected position of $(C_{60})Na_2^+$, $(C_{60})Na_3^+$ and $(C_{60})Na_7^+$ stable products.

clearly present in the case of native cations as shoulders on the left side of mass peaks. At the bottom of Figure 1, the typical mass spectrum obtained in reference [10] is also shown for further discussion (Fig. 1a). The spectroscopy of anionic species [17] was not performed here.

3.2 Photofragmentation of $(C_{60})Na_n^+$ and $(C_{60})_2Na_n^+$ clusters

Figure 2 shows photofragmentation mass spectra of size selected $(C_{60})Na_n^+$ clusters for $n = 3$ to 13. Only charged fragments are detected on the left side of photo-excited parents (shorter flight times). $(C_{60})Na_{n=1,2}^+$ clusters are very resistant to dissociation and their spectra are not displayed in this figure. For $(C_{60})Na_3^+$ up to $(C_{60})Na_8^+$, the dissociation pathways are consistent with the sequential evaporation of a neutral sodium atom. $(C_{60})Na_3^+$ is quite stable towards evaporation. From $(C_{60})Na_9^+$, clusters coated with an odd number of sodium atoms first evaporate a sodium dimer when even-numbered ones loose a monomer. The stepwise nature of the dissociation processes is confirmed by two main observations. First, the odd-even alternation in the dimer evaporation for the parent clusters is also retrieved for the fragments. For instance, $(C_{60})Na_{10}^+$ looses a monomer to give $(C_{60})Na_9^+$ that itself looses Na_2 to form $(C_{60})Na_7^+$, the rest of the sequence being consistent with the evaporation of monomers. Secondly, it has been checked that the extent of the fragment size distribution depends on the fluence of the fragmentation laser as expected for a sequential evaporative process [25]. With the fluence used to record these spectra, the dissociation sequences hardly go beyond $(C_{60})Na_3^+$ or $(C_{60})Na_2^+$ which shows the stability of these sizes. Only fragments still containing the C_{60} molecule are observed in Figure 2. Apparently, C_{60}^+ and Na_q^+ fragments ($q = 2$ to n) do not appear along the fragmentation process. We are able to detect only a small amount of Na^+ ions. Owing to the high laser fluence used here, they may be either the result of the re-ionization of Na atoms by the fragmentation laser or a trace of the re-evaporation of some hot Na_q^+ fragments that could have been directly emitted from the $(C_{60})Na_n^+$ clusters. In this case, Na_q^+ fragments would be hardly observed and it is not possible to conclude about this possibility. Anyhow, if such processes may exist, their contribution is certainly weak compared to the sequential evaporation of Na or Na_2.

The same experiments are performed on clusters containing two fullerene molecules. The photofragmentation spectra of $(C_{60})_2Na_n^+$ clusters with $n = 2$ to 17 are displayed in Figure 3. The right hand part of the figure shows a sequential evaporation of neutral Na atoms or Na_2 molecules. The competition between both processes now starts from $(C_{60})_2Na_{15}^+$ instead of $(C_{60})Na_9^+$ (see Fig. 2) with a very similar odd-even alternation. The most striking feature is the sudden stop of all the dissociation sequences at $(C_{60})_2Na_5^+$ which seems a particularly stable compound. We believe that no confusion can be made between the direct evaporation of one dimer ($(C_{60})_2Na_n^+ \rightarrow (C_{60})_2Na_{n-2}^+ + Na_2$) and a fast sequential evaporation of two atoms ($(C_{60})_2Na_n^+ \rightarrow (C_{60})_2Na_{n-1}^+ + Na \rightarrow (C_{60})_2Na_{n-2}^+ + 2Na$). Since the size to size relative intensities in a sequence of atom evaporations (see $(C_{60})_2Na_{n<15}^+$ for instance) are quite smooth, there is no reason for the $(C_{60})_2Na_{n-1}^+$ intermediate product to completely vanish to the benefit of $(C_{60})_2Na_{n-2}^+$, if the second process would hold. This remark is also valid for $(C_{60})Na_n^+$ clusters in Figure 2. The left part of Figure 3 also shows the appearance of fission products for which one of both C_{60} fullerenes has been evaporated. The most intense species is $(C_{60})Na_3^+$ but C_{60}^+, $(C_{60})Na_2^+$ and to a lesser extent $(C_{60})Na_4^+$ are also detected.

3.3 Unimolecular decomposition of $(C_{60})Na_n^+$ and $(C_{60})_2Na_n^+$ clusters

The preceding experiments have been performed on selected clusters initially photoionized with an ArF excimer laser. Even at low laser fluence, an extra internal energy is retained by the photoionized clusters because the photon energy is larger than the ionization potentials (more than 1.5–2 eV here, as inferred from the ionization thresholds in the next subsection). This additional warming is then sufficient for clusters to cool down through unimolecular evaporation processes during their free flight in the mass spectrometer (tenths of microseconds). Two pathways can occur: $(C_{60})Na_n^+ \rightarrow (C_{60})Na_{n-1}^+ + Na$ and $(C_{60})Na_n^+ \rightarrow (C_{60})Na_{n-2}^+ + Na_2$. The charged products are dispersed by the electrostatic reflector of the RTOFS and can be detected in the mass spectrum. As a consequence, three size distributions can be identified in the

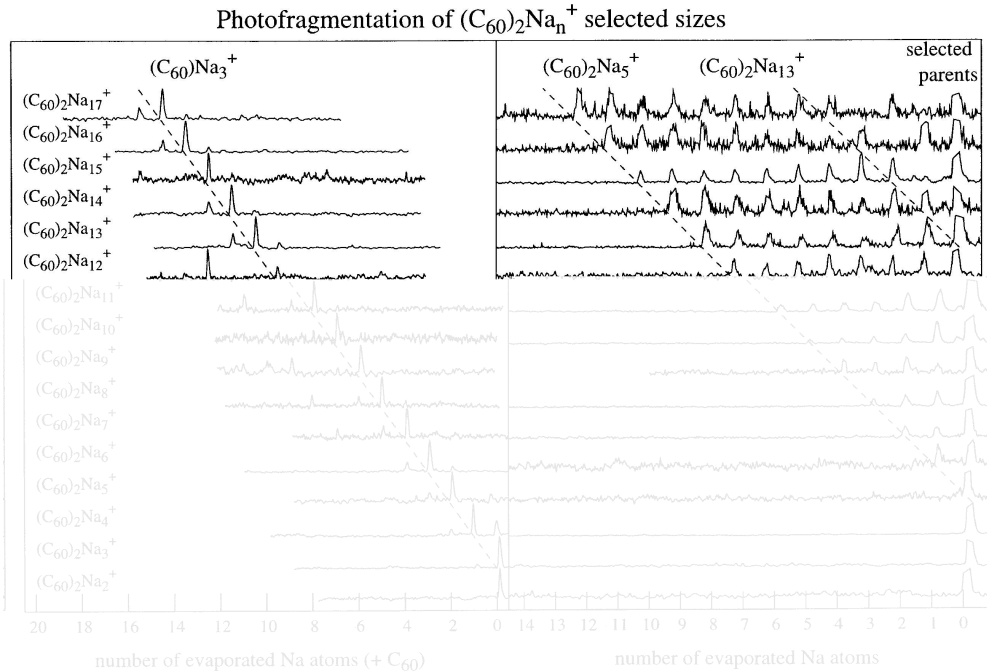

Fig. 3. Photofragmentation spectra of $(C_{60})_2Na_n^+$ clusters. Right side: region of the sequential evaporation of sodium atoms. The cut off of the evaporation sequences at $(C_{60})_2Na_5^+$ and the upper limit at $(C_{60})_2Na_{13}^+$ for the sequential monomer evaporation are indicated by an oblique line. Left side: region where at least one C_{60} molecule is evaporated. Oblique lines locate the position of the $(C_{60})Na_3^+$ products.

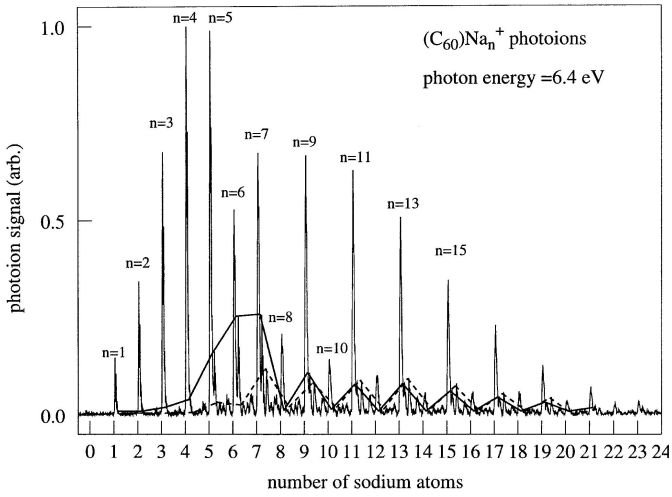

Fig. 4. Photoionization mass spectrum of $(C_{60})Na_n$ clusters at a photon energy of 6.4 eV. $(C_{60})Na_n^+$ photoionized clusters are able to evaporate Na atoms or Na_2 dimers to give $(C_{60})Na_{n-1}^+$ or $(C_{60})Na_{n-2}^+$ species. These products are detected on the right side of non-dissociated clusters of the same size (most intense peaks). They are connected here by a full line (atom evaporation) and a dashed line (dimer evaporation). The intensity of $(C_{60})Na_q^+$ product peaks must be compared to the intensity of non dissociated parent peaks containing one or two additional Na atoms depending on the evaporation pathway.

mass spectrum displayed in Figure 4. The first and most intense one corresponds to photoionized $(C_{60})Na_n^+$ clusters that have not evaporated neutral constituents during their flight towards the electrostatic reflector (undissociated parents). The second one corresponds to $(C_{60})Na_{n-1}^+$ products originating from the loss of a Na atom from some photoionized $(C_{60})Na_n^+$ clusters. Since this process occurs in the free flight towards the electrostatic mirror, the flight times of the products are close but slightly larger than those of undissociated clusters of the same size. The third one gives the $(C_{60})Na_{n-2}^+$ products whose peaks are approximately twice more shifted from undissociated cluster mass peaks of this size. To characterize a unimolecular evaporation process, the peak intensity of $(C_{60})Na_n^+$ products located close to the one of $(C_{60})Na_n^+$ undissociated clusters must rather be compared to the peak intensity of $(C_{60})Na_{n+1}^+$ or $(C_{60})Na_{n+2}^+$ undissociated sizes, depending on whether these products result from the evaporation of one or two Na atoms respectively. It is therefore possible to estimate the corresponding dissociation rates and the branching ratios between the monomer and the dimer evaporations. The results are displayed in Figure 5 (circles). The same measurements could be made on selected sizes by the use of a mass filter in the free flight zone but the first method is preferred because all the dissociation patterns are recorded in one single spectrum and all the sizes are heated under the same experimental conditions. This is important for a comparative analysis.

The unimolecular evaporation processes are basically the same as those previously discussed in high laser fluence photofragmentation experiments (Sect. 3.2). The main difference is that the overall evaporation efficiency is less important because less energy is stored within the clusters and mainly one evaporation step can be detected. A very

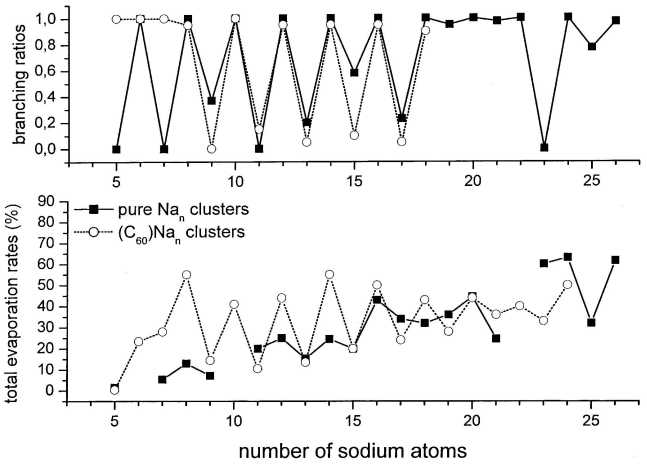

Fig. 5. Total evaporation rates $T_n = (I_{n-1}+I_{n-2})/(I_n+I_{n-1}+I_{n-2})$ (bottom) and branching ratios $Br_n = I_{n-1}/(I_{n-1}+I_{n-2})$ where I_n is the intensity of undissociated $(C_{60})Na_n^+$ clusters. I_{n-1} and I_{n-2} are the intensities of their fragments resulting from the evaporation of a Na atom or a Na_2 molecule respectively. The circles correspond to the data on $(C_{60})Na_n^+$ clusters measured from the spectrum in Figure 4 and the black squares are the results for pure sodium clusters from reference [33].

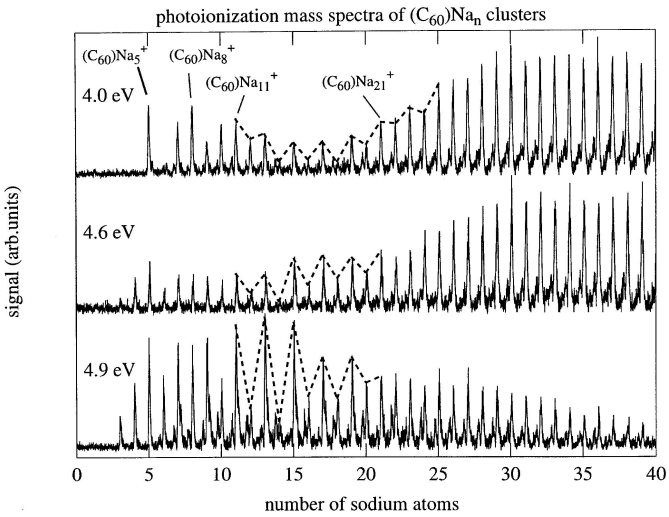

Fig. 6. Photoionization mass spectra of $(C_{60})Na_n$ clusters recorded at 4.92 eV (252 nm), 4.6 eV (270 nm) and 4 eV (308 nm). Mass peaks in the region of the odd-even alternation are connected by a dotted line to guide the eyes. Small peaks on the left side of the main $(C_{60})Na_n$ cluster peaks correspond to $(C_{60})Na_{n-1}O$ oxides or $(C_{60})Na_{n-1}OH$ hydroxides. The coverage with Na atoms is less important for the bottom spectrum.

strong odd-even alternation both in the total evaporation rates and the monomer-dimer branching ratios is observed from $(C_{60})Na_8^+$. Below $(C_{60})Na_4^+$, the dissociation rates are low and they are progressively increasing from $(C_{60})Na_5^+$ up to $(C_{60})Na_8^+$. Cations with an even number of attached sodium clusters are much more fragile than odd-numbered ones and essentially evaporate monomers since the latter evaporate dimers. Within the measurement accuracy, the branching ratios oscillate between values close to 0 or 1. The second point is that this behavior is apparent for sizes larger than $(C_{60})Na_7^+$. Small clusters only evaporate monomers. In the case of $(C_{60})_2Na_n^+$ clusters (not shown here), an odd-even alternation in the monomer-dimer branching ratios can also be detected from $(C_{60})_2Na_{15}^+$ together with traces of some fission products (mainly $(C_{60})Na_3^+$). The latter are less abundant as compared to photofragmentation experiments and are hardly measurable for sizes larger than $(C_{60})_2Na_8^+$.

3.4 Near threshold photoionization of $(C_{60})_mNa_n$ clusters

The preceding experiments are useful to understand the stability of cationic clusters. We have also recorded photoionization mass spectra at different photon energies and at low laser fluence to get information about the neutral cluster ionization potentials. A mass spectrum obtained with the ArF laser (6.4 eV) at moderate fluence (Fig. 1b) is found similar to the typical one displayed in Figure 1a and reported in reference [10]. As pointed out by these authors, it essentially reflects the stability of positive ions through fast evaporation processes following their heating in a multi-photon ionization scheme. Lowering the laser fluence, so as to reach a one-photon ionization regime, only slightly modifies the overall shape of the mass spectrum in Figure 1b. The odd-even alternations and sharp edges in the size distribution are slightly less marked but the photon energy is still too large as compared to ionization potentials for not inducing further evaporations that could misrepresent the exact size distribution of the photoionized clusters.

In Figure 6 are displayed three photoionization mass spectra of $(C_{60})Na_n$ clusters recorded at different photon energies, closer to their actual ionization potentials. The fluence is kept as low as possible to avoid evaporation events. At 4.9 eV or 4.6 eV, the spectra are quite similar. $(C_{60})Na$ and $(C_{60})Na_2$ are not detected. An odd-even alternation between $(C_{60})Na_{11}$ and $(C_{60})Na_{21}$ clearly appears in both spectra. In this size range, even-numbered clusters and especially $(C_{60})Na_{14}$ have higher ionization potential values as their odd neighbors. At 4 eV, the odd-even alternation is just slightly more pronounced and $(C_{60})Na_3$, $(C_{60})Na_4$ and $(C_{60})Na_6$ are now clearly absent. On the contrary, the signal for $(C_{60})Na_5$, $(C_{60})Na_8$ and $(C_{60})Na_{11}$ remains relatively strong. Figure 7 shows a photoionization mass spectrum recorded at a much lower photon energy (3.45 eV). Clusters are detected from about $(C_{60})Na_{15}$. An odd-even alternation ranges from this size up to $(C_{60})Na_{35}$ approximately. A step edge in the vicinity of $(C_{60})Na_{84}$ is clearly marked and weak steps in the mass distribution can also be detected and are indicated by star symbols about $(C_{60})Na_{35}$, $(C_{60})Na_{61}$ and $(C_{60})Na_{95}$.

It is not possible to extract precise cluster ionization thresholds from a few photoionization spectra, but rough values can nevertheless be inferred. Obviously, the ionization potentials (IP) of $(C_{60})Na_n$ clusters with $n \geq 4$ are of

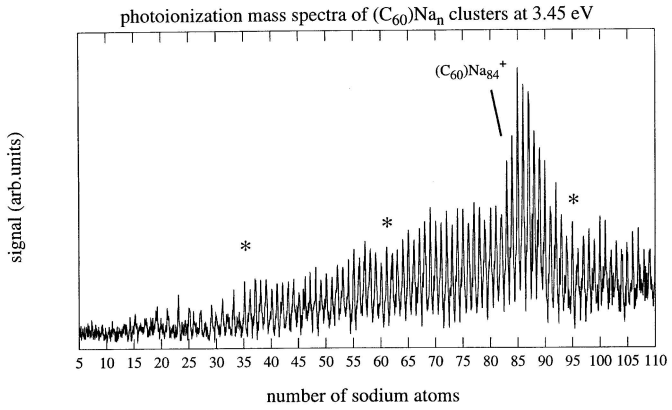

Fig. 7. Photoionization mass spectrum of $(C_{60})Na_n$ clusters recorded at 3.45 eV (360 nm). The main feature is the relatively large signal above $(C_{60})Na_{84}$. The stars indicate some minor anomalies in the size distribution about $n = 35$, 61 or 95.

the same order as those measured [26,27] or calculated [28] for pure sodium clusters and globally range between 3.5 and 4 eV even if even-numbered $(C_{60})Na_{14}$, $(C_{60})Na_{16}$ and $(C_{60})Na_{18}$ clusters seem to have low photoionization cross-sections at these photon energies. This behavior has been recently shown by Nagao *et al.* [29] in the case of holmium coated C_{60}. These authors explain the lowering of the IP for $(C_{60})Ho_n$ clusters as compared to the one of C_{60} by the efficient electron transfer from the metal atoms to the lowest unoccupied orbitals (LUMO) of the fullerene. Here, it is more surprising to notice that $(C_{60})Na$, $(C_{60})Na_2$ and $(C_{60})Na_3$ have clearly much larger IP values than pure sodium clusters. This can be related to the high stability of their cations as discussed in Section 3.2.

4 Discussion

4.1 The stability of $(C_{60})_mNa_n^+$ clusters

Photoionization mass spectroscopy of $(C_{60})_mNa_n$ complexes has been extensively performed by Martin *et al.* [2,10]. As illustrated in Figure 1a, their spectra obtained at high ionization fluence give the size distribution after ionization and stabilization through all the possible dissociation pathways. This differs from our experiments in the sense that such spectra only picture the final result of the cluster fragmentation sequences. These authors mainly observe the formation of not very structured groups of sizes with compositions ranging from $(C_{60}Na_2)_mNa^+$ to $(C_{60}Na_6)_mNa^+$ and a relative high intensity for $(C_{60}Na_4)_mNa^+$ clusters. In each of the size distributions of clusters containing one, two and three C_{60} fullerenes, a strong odd-even alternation is visible after $(C_{60}Na_6)_{m=1,2,3}Na^+$. The clusters containing an even number of sodium atoms being less abundant than odd ones as clearly seen in Figure 1a.

This can be compared to our photoionization mass spectrum of Figure 1b. Here the size effects are less pronounced than in Figure 1a because the laser fluence is kept lower. Owing the high density of the neutral cluster beam, it is not possible to increase the laser fluence in a comparable way because of a spurious blurring of the mass spectra induced by space charge effects in the ionization region. The same qualitative trends are nevertheless observed. The strong odd-even alternation in the $(C_{60})Na_n$ group is not only the result of fluctuations in size to size stabilities but also reflects here the high ionization thresholds of the even $(C_{60})Na_n$ clusters with $n \geq 8$ (see also Figs. 6 and 7). It is interesting to notice that, depending on the source settings, native cations can display close but not so strong features. The spectrum in Figure 1c is the more structured one that can be obtained here. Typical spectra of native cations are generally smoother and magic sizes of high stability are not clearly detected.

The results of our photofragmentation study on selected sizes presented in the previous section are fully consistent with the mass spectrum of reference [10]. The relatively high dissociation rates detected for $(C_{60})Na^+_{2n\geq 8}$ and $(C_{60})_2Na^+_{2n\geq 14}$ clusters and the preferential evaporation of dimers from $(C_{60})Na^+_{2n+1\geq 9}$ and $(C_{60})_2Na^+_{2n+1\geq 15}$ both account for the strong odd-even alternation observed in the mass spectrum in Figure 1a. Moreover, the sharp edges at the beginning of the size distributions detected at $(C_{60})Na_3^+$ and $(C_{60})_2Na_5^+$ are clearly consistent with the results of Figures 2 and 3. The relatively stable $(C_{60})Na_3^+$ cluster acts as a bottleneck in the dissociation sequences of larger $(C_{60})Na_n^+$ sizes (Fig. 2) and is also a preferential fission product from $(C_{60})_2Na_n^+$ clusters (Fig. 3). The stopping of the evaporation sequences of $(C_{60})_2Na_n^+$ clusters at $(C_{60})_2Na_5^+$ (Fig. 3) also explains why this size is the first to be detected in the high fluence photoionization mass spectrum of the $(C_{60})_2Na_n^+$ group [10].

4.2 The structure of $(C_{60})_mNa_n^+$ clusters

At this point, one can try to speculate about the structure of these clusters. In reference [10], a sharp edge in the size distribution of $(C_{60})_3Na_n^+$ clusters is measured at $n = 7$ with the recurring odd-even-alternation starting now from $(C_{60})_3Na_{19}^+$ (see Fig. 1a). This feature can also be guessed in some of our mass spectra. We were not able to measure the photofragmentation processes in $(C_{60})_3Na_n^+$ clusters but we may reasonably suppose from reference [10] that $(C_{60})_3Na_7^+$ should behave like $(C_{60})_2Na_5^+$ (as seen in Fig. 3) and that an odd-even alternation in the branching ratios between the dimer and the monomer evaporation would be expected from $(C_{60})_3Na_{21}^+$. This would explain the odd-even alternation in abundance mass spectra from $(C_{60})_3Na_{19}^+$. On this assumption, the comparison between the three size groups: $(C_{60})Na_n^+$, $(C_{60})_2Na_n^+$ and $(C_{60})_3Na_n^+$ first indicates a shift of six sodium atoms at the onsets of the odd-even effects ($(C_{60})Na_9^+$, $(C_{60})_2Na_{15}^+$ and $(C_{60})_3Na_{21}^+$ for the first dimer evaporation) and a shift of two sodium atoms for the step edges in the size distributions ($(C_{60})Na_3^+$, $(C_{60})_2Na_5^+$ and $(C_{60})_3Na_7^+$).

Concerning the six atom bunching, it was initially proposed by Martin *et al.* that the first six adsorbed sodium

atoms were likely to transfer one electron to the six-fold degenerate LUMO of the fullerene [10]. Such an ionic bonding would induce the electrostatic repelling of these atoms that are located as far as possible one from each other. The $(C_{60})Na_6$ neutral entity (or $(C_{60})Na_7^+$ if positively charged) is then expected to be a stable closed shell molecule. If the hypothesis about a so strong charge transfer process may be questioned from theoretical calculations, the singularity of this particular size must be inevitably invoked to rationalize the measured cluster stabilities. We also believe that the cations $(C_{60})Na_7^+$, $(C_{60})Na_6(C_{60})Na_7^+$ and $(C_{60})Na_6(C_{60})Na_6(C_{60})Na_7^+$ are basic units from which larger clusters as $(C_{60})Na_{n>7}^+$, $(C_{60})_2Na_{n>13}^+$ and $(C_{60})_3Na_{n>19}^+$ will grow. In clusters containing more than one fullerene and assuming that the Na–C_{60} bonds are ionic in nature, the sodium atoms are unlikely to participate to strong inter-fullerene links. We will assume that C_{60} molecules are rather bonded through a [2+2] cycloaddition which is strong enough (1.25 eV) to ensure their polymerization [30]. To support this statement, it would be useful to consider the relative stability of the sodium bridged $(C_{60})Na(C_{60})$ dimer and the $(C_{60})_2$ cycloadduct. Only a theoretical estimation can be made in the absence of experimental data on the sodium compound. Ignoring activation barriers and considering the most favorable dissociation channel: $(C_{60})Na(C_{60}) \rightarrow (C_{60})Na+C_{60}$, the sodium bridged dimer is found to be bound by 0.68 eV compared to 1.15 eV for the $(C_{60})_2$ cycloadduct and is obviously less stable. As detailed in a previous paper [31], these DFT (density functional theory) calculations have been performed within the local density approximation (LDA), adopting a pseudo-potential approach to describe the core electrons of carbon and sodium atoms and allowing a structural relaxation for the clusters.

4.2.1 The $(C_{60}Na_6)_mNa_{n>1}^+$ clusters

The physical origin of the odd-even alternation in the evaporation of monomers or dimers is an important issue. Let us consider the case of positive clusters containing one C_{60}. Two scenarios can be proposed both assuming that the first seven atoms (six for the neutral) are ionically bounded to the fullerene and behave as positive "ions". The first hypothesis (model I) is to envisage this odd-even alternation as a pairing effect similar to what is observed in pure metallic sodium clusters. In this case, the $n-7$ extra atoms in a $(C_{60})Na_n^+$ cluster are expected to group around a single Na^+ ion and form a small Na_{n-6}^+ metallic cluster at the surface of C_{60}. With regard to experiment, the formation of a single close-packed sodium droplet is certainly the most favorable situation on energetic grounds. As a matter of fact, a random nucleation around any of the six Na^+ ions would inevitably prevent the appearance of a clear odd-even alternation in the mass spectra. Upon photoexcitation, the sodium droplet will almost evaporate like a pure sodium one [32–34]. In this ideal scheme, the Na_{n-6}^+ metallic cluster can be considered as weakly perturbed by the C_{60} and the other six isolated atoms. A more complex situation, for instance an odd or a non integer charge transfer from the sodium droplet to the C_{60}, is unlikely to produce such a sharp odd-even alternation having also the correct order (pure even and odd positive sodium clusters evaporate mainly Na and Na_2 respectively [33,34]). A second scenario proposed by Martin *et al.* [10] would be that the extra sodium atoms join each of the seven "ions" so as to form Na_3^+ trimers that are known to be very stable species (model II). In $(C_{60})Na_{7+2q}^+$ clusters, the sodium atoms will be adsorbed in the form of $7-q$ Na^+ ions and q Na_3^+ trimers. $(C_{60})Na_{7+2q-1}^+$ clusters will contain an isolated Na_2^+. In photoexcited odd numbered clusters, a Na_3^+ molecule will evaporate a neutral dimer so as to leave the Na^+ ion. In even-numbered clusters, this is the isolated Na_2^+ molecule that will much more easily loose one atom to leave Na^+. Here, the odd-even alternation is mainly of geometric origin, depending on the formation of Na_3^+ islands. This scheme is valid up to the completion of about seven trimers ($q = 7$).

The onsets of the odd even-alternation for clusters containing one, two or three C_{60} can be explained by each of both mechanisms. If the basic units are actually the $(C_{60})Na_7^+$, $(C_{60})Na_6(C_{60})Na_7^+$ and $(C_{60})Na_6(C_{60})Na_6(C_{60})Na_7^+$ cations as proposed above, the hypothesis of the formation of stable Na_3^+ islands (model II) will be effective for $(C_{60})Na_n^+$, $(C_{60})_2Na_n^+$ and $(C_{60})_3Na_n^+$ clusters as soon as $n \geq 9$, 15 and 21 respectively. The 7, 13 or 19 first sodium atoms that are ionically bonded to C_{60}, $(C_{60})_2$ or $(C_{60})_3$ will act as independent nucleation sites for the Na_3^+ islands. In model I, an isolated metallic droplet can be formed on a particular C_{60} fullerene and probably the one that carries the positive charge ($(C_{60})Na_7^+$ unit). The gathering of extra sodium atoms in one place is not impossible owing to their high mobility at the surface of C_{60} [18,35] and their ease to move from one fullerene to another in the region of a [2+2] link [36]. In this case, the growth occurs on one single C_{60} whatever the number of other fullerenes in the cluster.

4.2.2 The $(C_{60}Na_2)_mNa^+$ clusters

Following the above assumption for the structure of the $(C_{60})Na_7^+$, $(C_{60})Na_6(C_{60})Na_7^+$ and $(C_{60})Na_6(C_{60})Na_6(C_{60})Na_7^+$ basic units, we may also propose an explanation for the step edges of the size distributions observed at $(C_{60})Na_3^+$, $(C_{60})_2Na_5^+$ and $(C_{60})_3Na_7^+$. $(C_{60})Na_3^+$ is obviously a relatively stable cluster (see Fig. 2) and its neutral isoelectronic counterpart $(C_{60})Na_2$ should present a similar stability [20]. When dissociating, the $(C_{60})_2Na_n^+$ clusters first loose the extra atoms added to the basic $(C_{60})Na_6(C_{60})Na_7^+$ unit that will carry on evaporating atoms until $(C_{60})_2Na_5^+$ is reached (see Fig. 3). Then, if sodium atoms are randomly evaporated, the most probable arrangement for this cluster will be $(C_{60})Na_2(C_{60})Na_3^+$. At this point and owing to the stability of the two subparts, it appears more favorable to break the inter-fullerene bond than to evaporate a next atom from $(C_{60})Na_2$ or $(C_{60})Na_3^+$. The corresponding

dissociation energy must then be larger than the energy required to severe the [2+2] cycloaddition link estimated about 1.25 eV [30]. This explains the observation of $(C_{60})Na_3^+$ as a major fission product in Figure 3. The presence of other fission products can be the signature of different but minor dissociation sequences (Sect. 3.2). Even if the C_{60}^+ product may result form the further evaporation of the $(C_{60})Na_n^+$ fission products themselves, we have no clear interpretation for its relatively high intensity in the case of $(C_{60})_2Na_{12}^+$ (Fig. 3) since all the $(C_{60})_2Na_n^+$ clusters have been photoexcited at close laser fluences. Nevertheless, if the scenario proposed for the fragmentation of $(C_{60})_2Na_n^+$ clusters is valid, the lowest size in the dissociation sequence of $(C_{60})_3Na_n^+$ clusters should be $(C_{60})Na_2(C_{60})Na_2(C_{60})Na_3^+$, namely $(C_{60})_3Na_7^+$. Unfortunately, this was not measured in this study but could explain the enhancement of $(C_{60})_3Na_7^+$ in the mass spectrum of Figure 1 (bottom trace) and also the possible stepwise formation of $(C_{60})Na_3^+$ and $(C_{60})_2Na_5^+$ through the fission of $(C_{60})Na_2(C_{60})Na_2(C_{60})Na_3^+$.

It is important to note that, contrary to rubidium and potassium [2,10], $(C_{60}Na_6)Na^+$ is not exceptionally stable (see also Fig. 1). Besides $(C_{60})Na_7^+$, other sizes like $(C_{60})Na_5^+$ and specially $(C_{60})Na_3^+$ present marked stabilities. As for $(C_{60})Na_3^+$ and $(C_{60})Na_2$, $(C_{60})Na_5^+$ and $(C_{60})Na_4$ could be at the origin of the relative stability of $(C_{60})Na_4(C_{60})Na_4\ldots(C_{60})Na_5^+$ complexes that would act as intermediate bottleneck sizes in the fragmentation sequences. This is consistent with the observation of a slight enhancement of $(C_{60}X_4)_nX^+$ clusters in the photoionization mass spectra of sodium or even potassium coated fullerenes [10].

4.2.3 The large $(C_{60})_mNa_{n\gg m}^+$ clusters

The results of photofragmentation experiments are roughly consistent with both mechanisms evoked for the growth of $(C_{60})Na_n^+$ clusters (models I and II) and do not allow to settle this issue. The study of more largely coated fullerenes should give more information since the arrangement of sodium atoms is expected to be different in each case. In model I, the sodium droplet is formed early. It will continue to grow further in such a way that the large $(C_{60})Na_n^+$ clusters can be considered as a sodium cluster attached to the C_{60}, eventually decorated with a few adsorbed and isolated sodium atoms. In model II, the Na_3^+ island formation will be complete for $n = 7 \times 3 = 21$ or $n = 6 \times 3 = 18$ sodium atoms for positive or neutral clusters respectively. These values are close to the number of sodium atoms needed to form a complete shell around C_{60} assuming the formation of a triangular paving with a mean interatomic distance of 3.6 Å [28] and a shell radius of about 5.8 Å [11,19]. When the compacity of this shell is maximum, the full delocalization of the sodium conduction electrons and the metallic behavior can occur. The slightly weaker odd-even alternation observed after $n = 21$ in reference [10] is interpreted by the authors as a change in the nature of this effect: a transition from the geometric stability of Na_3^+ units towards a pairing of delocalized electrons in a metallic shell.

Photoionization mass spectroscopy can give information about each of both possibilities (shell or droplet). For instance, it has been proposed for $(C_{60})Cs_n$ clusters that cesium atoms wet the C_{60} surface and form an exterior concentric metallic shell. Their photoionization mass spectroscopy indicates the existence of an electronic shell structure qualitatively explained in the framework of a jellium model applied to a core-shell arrangement [5]. The shell closings are sharp and slightly different from those expected in the spherical jellium model applied to pure cesium clusters [5,7]. They are detected at $n = 27$, 33, 44, 61 or 98 for instance. Inspecting mass spectra of Figures 6 and 7, it is difficult to bring out similar effects even if some step edges about $n = 35$, 61 and 95 can be guessed. The only strong effect at $n = 84$ in Figure 7 is not explainable in this framework. Considering both experimental observations on cesium coated fullerenes and the calculation of their electronic shell closings assuming a transfer of six electrons to C_{60}, the absence of sharp electronic shell closures in the near-threshold photoionization mass spectra is an indication of a low symmetry for the metallic sodium island and seems to come against the hypothesis of a perfect wetting of the C_{60} surface by a sodium shell.

The second possibility from model I is less conflicting with experiment. If a sodium cluster is formed at the fullerene surface and therefore rules the geometric and electronic structures of this complex, the latter cannot be simply deduced from those of a pure sodium droplet. The attachment of the C_{60} will certainly perturb the effective potential experienced by the metal conduction electrons and breaks its spherical symmetry. In the absence of more precise calculations, the shell effect at $n = 84$ cannot be directly compared to the closest spherical jellium predictions at $n = 58$ or 92 for instance [37], even if the shell closings were corrected from the number of electrons that may be transferred to the C_{60}. If the effects of a symmetry lowering for the sodium cluster cannot be easily quantified, they are however responsible for very specific qualitative trends that are compatible with experimental observations. The splitting up of the electronic level degeneracy as compared to the spherical symmetry can explain the smoothing of the electronic shell closings that are indeed difficult to observe in near-threshold photoionization spectra (Figs. 6 and 7). Moreover, this is also consistent with the strong enhancement of the electron pairing effects that rule the very sharp odd-even alternations in the ionization properties (Figs. 6 and 7) of these clusters and in their relative stabilities (Figs. 1, 2 and 4). This is obvious from a comparison between the unimolecular evaporation rates and the monomer-dimer evaporation branching ratios measured on $(C_{60})Na_n^+$ or pure Na_n^+ clusters [33] as shown in Figure 5. The experimental conditions and the two evaporative ensembles are different but the overall evaporation rates are similar and a qualitative comparison is relevant. Up to $n \cong 20$, the dissociation rates and their odd-even fluctuations are much more marked for C_{60} coated clusters than for pure sodium ones. The same

observation can be made about the contrast in the odd-even alternation for the branching ratios. The values for $(C_{60})Na^+_{n>18}$ are not drawn in Figure 5 because of a low accuracy but they are estimated to strongly oscillate in a region where pure sodium clusters do not display such marked effects.

Other experimental and theoretical studies are in favor of such a description. Actually, polarizability measurements by Dugourd *et al.* [18] on C_{60} coated with sodium show a large electric dipole for neutral $(C_{60})Na_n$ clusters, even beyond $n = 20$. This result cannot be explained by a perfect core-shell arrangement that would not carry any permanent electric dipole moment. It is a strong indication for the progressive formation of a sodium bump that would be free to skate onto the fullerene surface [18,35]. Roques *et al.* [22] have recently performed calculations of the optimized geometries of a fullerene coated with many sodium atoms. They use an empirical potential method allowing the exploration of a large number of structures and show the formation of a sodium droplet as soon as eight sodium atoms are attached to C_{60}. This droplet is growing further when more sodium atoms are added.

5 Summary and conclusion

This study confirms that the bonding of Na atoms onto the C_{60} fullerenes is strongly modified after the earliest steps of the alkali atom attachment. The first six adsorbed atoms are certainly able to easily transfer electrons to the C_{60} molecules. This gives rise to a bonding which should be ionic in nature as proposed earlier [10]. The C_{60} molecule is likely to accommodate six potassium or rubidium atoms [2,10] which shows the relevance of the charge transfer mechanism and the ionic nature of the bonding for these elements. In the case of lithium, the bonding has an enhanced covalent character and lithium-coated C_{60} clusters a very different structure [13]. Sodium represents an intermediate situation. The special behavior of $(C_{60})Na^-_3$, $(C_{60})Na^-_6$, $(C_{60})Na^-_9$ that possess a relatively high electron affinity [16,17] is an illustration of the difficulty to apply the simple model where the fullerene would be considered as a mere electron pump for each of the six first sodium adatoms. The apparently low ionization potential values for $(C_{60})Na_5$, $(C_{60})Na_8$ and $(C_{60})Na_{11}$, as observed in Figure 6, mirror the results of photoelectron spectroscopy since these clusters exactly contain one more electron as $(C_{60})Na^-_3$, $(C_{60})Na^-_6$, $(C_{60})Na^-_9$.

If the coverage of C_{60} with up to six Na atoms is obviously special, the mechanism of charge transfer between the C_{60} and the sodium atoms looks quite subtle. The strength of the ionic bonding is decreasing when the number of transferred electrons is increasing. This is illustrated by the present experimental results where the stability of $(C_{60})Na^+_7$ (or $(C_{60})Na_6$) is not found to be especially high as compared to smaller sizes as $(C_{60})Na^+$, $(C_{60})Na^+_2$, $(C_{60})Na^+_3$ for instance. This can be also recovered in the ionization potential values for these sizes and in the cohesiveness of $(C_{60})Na_2$ and $(C_{60})Na^+_3$as compared to the [2+2] cycloaddition link of C_{60} molecules, as observed in the high fission probability of the $(C_{60})_2Na^+_5$ compound. The bonding remains mainly ionic in nature up to the transfer of about six electrons, even if the rough hypothesis of a complete filling of the six-fold degenerated and frozen LUMO of the C_{60} is certainly by too simple. This is supported by the theoretical work of Hamamoto *et al.* devoted to the electronic and geometric properties of M_2C_{60}, M_3C_{60}, M_6C_{60} and $M_{12}C_{60}$ with M = Li, Na and K [21]. Even if these DFT calculations ignore the relaxation of the C_{60} cage, they clearly show the importance of charge transfer from the alkali atoms to the C_{60} and how this influences their repulsion or their possible bonding. A global transfer close to six electrons for $(C_{60})Na_6$ and $(C_{60})Na_{12}$ can be inferred from this study. It appears that increasing the number of alkali atoms also makes their bonding more favorable by reducing the strength of the electrostatic repulsion that originates from the charge transfer process. In this respect, the cluster state of charge is of main importance: for a given size, metal-metal bonds are more likely for anions than for neutrals and for cations. Some indications for the formation of sodium trimers at the fullerene surface can be found up $(C_{60})Na^+_{21}$ in the mass spectroscopy study by Martin *et al.* [10] or up to $(C_{60})Na^-_{12}$ in the photoelectron spectroscopy experiments of Palpant *et al.* [16,17]. It must be noticed that in the case of anions, the formation of sodium trimers does not seem to require the preliminary attachment of six isolated atoms as for cations. The formation of Na_3 islands is not turned out by the results of Hamamoto *et al.* [21], especially in the case of $(C_{60})Na_{12}$ even if all the possible configurations have not been explored for this size. The weakening of ionic bonding and electrostatic repulsion when adding more and more sodium atoms is also obvious in the theoretical study of Roques *et al.* [22]. When the cluster size is increasing, the number of isolated atoms that do not belong to the sodium droplet is decreasing from 5 for $(C_{60})Na_8$ down to 3 for $(C_{60})Na_{20}$ and maybe less for larger sizes. This shows that the formation of the sodium bump and its bonding to the fullerene strongly modify the cluster structure by altering the ionic bonds and the charge transfer mechanism. A simple picture of the latter can be valid in the first stages of the coverage with sodium atoms. Obviously, the exact structure of $(C_{60})Na_n$ clusters as a function of their charge state and in the range $n = 6$ to 12 remains an open issue.

C_{60} molecules coated with six sodium atoms (seven for the cations) appear as basic units for the further growth of larger clusters whatever the number of fullerene molecules in the complexes. The behavior of much larger sizes can be explained by the building of a sodium entity where a metallic bonding dominates. Is it a continuous shell around the fullerene or an isolated droplet that more weakly wets the fullerene surface? This study is rather in favor of an entity of low symmetry. In the absence of electronic shell calculations for a more or less deformed metallic droplet attached to an impurity made of a bare or a partially sodium-coated C_{60} molecule, no definitive conclusions can be drawn. This hypothesis is nevertheless

strengthened by recent experimental and theoretical studies [18,22] and is consistent with experimental observations concerning the presence of strong odd-even alternations and the absence of a sharp electronic shell fillings at the predicted sizes. The actual morphology of sodium coated C_{60} is certainly intermediate between two extreme situations corresponding to a full segregation process or a complete wetting of the fullerene surface. The initial decoration of the C_{60} surface with several isolated sodium atoms is induced by the ionic nature of the bonding in the first steps of the coverage and a metallic cluster can develop as soon as the metal-metal bonds become more favorable. Moreover, we have to consider that the atoms can easily move at the fullerene surface at room temperature [35]. This motion can explain why the models based on static geometric structures are too naive pictures. It may also play an important role in the observed electric susceptibilities in neutral $(C_{60})Na_n$ clusters for small n values, as recently demonstrated in the case of the $[PABA]_2$ (Para-Amino-Benzoic-Acid) molecule [38].

The authors are grateful to F. Spiegelman, F. Calvo, R. Antoine, Ph. Dugourd and D. Rayane for helpful discussions.

References

1. *Fullerenes: Chemistry, Physics, and Technology*, edited by K.M. Kadish, R.S. Ruoff (John Wiley & Sons Inc., NewYork, 2000) and references therein
2. U. Zimmermann, N. Malinowski, A. Burkhardt, T.P. Martin, Carbon **33**, 995 (1995)
3. F. Tast, N. Malinowski, M. Heinebrodt, I.M.L. Billas, T.P. Martin, J. Chem. Phys. **106**, 9372 (1997)
4. U. Zimmermann, N. Malinowski, U. Näher, S. Franck, T.P. Martin, Phys. Rev. Lett. **72**, 3542 (1994)
5. M. Springborg, S. Satpathy, N. Malinowski, U. Zimmermann, T.P. Martin, Phys. Rev. Lett. **77**, 1127 (1996)
6. S. Frank, N. Malinowski, F. Tast, M. Heinebrodt, I.M.L. Billas, T.P. Martin, Z. Phys. D **40**, 250 (1997)
7. P. Mierzyński, K. Pomorski, Eur. Phys. J. D **21**, 311 (2002)
8. A. Rubio, J.A. Alonso, J.M. López, M.J. Stott, Phys. Rev. B **49**, 17397 (1994)
9. P. Weis, R.D. Beck, G. Bräuchle, M.M. Kappes, J. Chem. Phys. **100**, 5684 (1994)
10. T.P. Martin, N. Malinowski, U. Zimmermann, U. Näher, H. Schaber, J. Chem. Phys. **99**, 4210 (1993)
11. D. Östling, A. Rosén, Chem. Phys. Lett. **281**, 352 (1997)
12. D. Östling, A. Rosén, Chem. Phys. Lett. **202**, 389 (1993)
13. U. Zimmermann, A. Burkhardt, N. Malinowski, U. Näher, T.P. Martin, J. Chem. Phys. **101**, 2244 (1994)
14. J. Kohanoff, W. Andreoni, M. Parinello, Chem. Phys. Lett. **198**, 472 (1992)
15. T. Aree, T. Kerdchaoren, S. Hannongbua, Chem. Phys. Lett. **285**, 221 (1998)
16. B. Palpant, A. Otake, F. Hayakawa, Y. Negishi, G.H. Lee, A. Nakajima, K. Kaya, Phys. Rev. B **60**, 4509 (1999)
17. B. Palpant, Y. Negishi, M. Sanetaka, K. Miyajima, S. Nagao, K. Judai, D.M. Rayner, B. Simard, P.A. Hackett, A. Nakajima, K. Kaya, J. Chem. Phys. **114**, 8459 (2001)
18. Ph. Dugourd, R. Antoine, D. Rayane, I. Compagnon, M. Broyer, J. Chem. Phys. **114**, 1970 (2001)
19. A.S. Hira, A.K. Ray, Phys. Rev. A **52**, 141 (1995)
20. A.S. Hira, A.K. Ray, Phys. Rev. A **54**, 2205 (1996)
21. N. Hamamoto, J. Jitsukawa, C. Satoko, Eur. Phys. J. D **19**, 211 (2002)
22. J. Roques, F. Calvo, F. Spiegelman, C. Mijoule, Phys. Rev. Lett. **90**, 75505 (2003)
23. M. Pellarin, C. Ray, J. Lermé, J.L. Vialle, M. Broyer, P. Melinon, J. Chem. Phys. **112**, 8436 (2000)
24. C. Ray, M. Pellarin, J. Lermé, J.L. Vialle, M. Broyer, X. Blase, P. Mélinon, P. Kéghélian, A. Perez, J. Chem. Phys. **110**, 6927 (1999)
25. C. Bréchignac, Ph. Cahuzac, N. Kebaïli, J. Leygnier, A. Sarfati, Phys. Rev. Lett. **68**, 3916 (1992)
26. M.L. Homer, J.L. Persson, E.C. Honea, R.L. Whetten, Z. Phys. D **22**, 441 (1991)
27. M.M. Kappes, M. Schär, U. Röthlisberger, C. Yeretzian, E. Schumacher, Chem. Phys. Lett. **143**, 251 (1988)
28. V. Bonačić-Koutecký, P. Fantucci, J. Koutecký, Phys. Rev. B **37**, 4369 (1988)
29. S. Nagao, Y. Negishi, A. Kato, Y. Nakamura, A. Nakajima, K. Kaya, J. Chem. Phys. **117**, 3169 (2002)
30. Y. Wang, J.M. Holden, X.X. Bi, P.C. Ecklund, Chem. Phys. Lett. **217**, 413 (1994)
31. M. Pellarin, E. Cottancin, J. Lermé, J.L. Vialle, M. Broyer, F. Tournus, B. Masenelli, P. Mélinon, J. Chem. Phys. **117**, 3088 (2002)
32. C. Bréchignac, Ph. Cahuzac, J.Ph. Roux, D. Pavolini, F. Spiegelmann, J. Chem. Phys. **87**, 5694 (1987)
33. C. Bréchignac, Ph. Cahuzac, J. Leygnier, J. Wiener, J. Chem. Phys. **90**, 1492 (1989)
34. V. Bonačić-Koutecký, I. Boustani, M. Guest, J. Koutecký, J. Chem. Phys. **89**, 4861 (1988)
35. D. Rayane, R. Antoine, Ph. Dugourd, E. Bénichou, A.R. Allouche, M. Aubert-Frécon, M. Broyer, Phys. Rev. Lett. **84**, 1962 (1999)
36. From different theoretical studies the distance from one adsorbed sodium atom to the fullerene surface is estimated about 2–2.5 Å [11,19,21]. This value is larger or of the order of the surface to surface distance between two fullerenes involved in a [2+2] cycloaddition link
37. M.L. Cohen, M.Y. Chou, W.D. Knight, W.A. de Heer, J. Chem. Phys. **91**, 3141 (1987)
38. I. Compagnon, R. Antoine, D. Rayane, M. Broyer, Ph. Dugourd, Phys. Rev. Lett. **89**, 253001 (2002)